Protein-Inorganic Conjugates

Synthesis and Self-Assembly of Organoclay-Wrapped Biomolecules**

*Avinash J. Patil, Eswaramoorthy Muthusamy, and Stephen Mann**

Protein-based nanostructures are expected to play a key role in the development of multifunctional materials and devices for bio-nanotechnological applications.[1–3] Although proteins excel in functional specificity, their structural and chemical sensitivity to ambient conditions can seriously compromise the use and integration of such macromolecules in diverse applications. Although there are numerous reports on the enhanced thermal and chemical stability of proteins by immobilization on surfaces[4–8] or within matrices such as amorphous gels[9–11] and layered solids,[12,13] the wrapping of individual protein/enzyme molecules with inorganic materials to produce functionally isolated hybrid nanoparticles has not been reported. Herein we describe investigations that strongly suggest that individual molecules of met-myoglobin (Mb), haemoglobin (Hb) or glucose oxidase (GOx) can be wrapped with an ultrathin shell of an aminopropyl-functionalized magnesium (organo)phyllosilicate to produce aqueous dispersions of discrete protein–inorganic nanoparticles. Similar procedures but with organoclay oligomers that have pendent long-chain hydrophobic moieties result in self-assembly of the protein–inorganic nanoparticles into higher-order superstructures. In each case, the encapsulated proteins are structurally and functionally intact and show enhanced thermal stability up to temperatures of 85 °C.

In general, "armour-plated" protein/enzyme molecules were prepared by mixing solutions of Mb, Hb, or GOx with aqueous solutions containing oligomers of a positively charged exfoliated organoclay (Figure 1). The organoclay was prepared by chemical synthesis[14,15] (see Experimental Section) and consisted of a highly disordered talclike 2:1 trioctahedral smectite structure with a central brucite sheet of octahedrally coordinated MgO/OH chains overlaid on both sides with an aminopropyl-functionalized silicate network to give an approximate unit cell composition of $[H_2N(CH_2)_3]_8Si_8Mg_6O_{16}(OH)_4$. Protonation of the amino groups by dispersion of the clay in water resulted in exfoliation and partial disintegration of the organoclay layers into cationic oligomers that were fractionated by gel chromatography to produce stable transparent sols that were subsequently added to protein/enzyme solutions.

For each protein/enzyme investigated, TEM studies showed the presence of discrete electron-dense nanoparticles randomly arranged across the support film of the grid (Figure 2a–c). EDX analysis for samples prepared in the presence of Mb or Hb, confirmed that the nanoparticles comprised both protein (Fe, S) and organoclay (Si, Mg, Cl) species (Figure 2d). In general, the nanoparticles were spheroidal and monodisperse in size with mean dimensions of 4.0 nm ($\sigma = 0.6$ nm), 7.8 nm ($\sigma = 0.8$) and 6.4 ($\sigma = 0.9$ nm) for Mb, Hb and GOx samples, respectively. The variation in nanoparticle size showed a direct correlation with the respective molecular dimensions of the different proteins/enzyme (Mb, $4.5 \times 3.5 \times 2.5$ nm; Hb, $6.5 \times 5.4 \times 5.3$ nm; GOx, $6.0 \times 5.2 \times 3.7$ nm), which suggests that each nanoparticle consisted of a single biomolecule wrapped by a continuous sheet of condensed organoclay oligomers. Significantly, no organoclay nanoparticles were observed in the absence of the proteins or enzyme, suggesting that condensation of the magnesium (aminopropyl)phyllosilicate oligomers was specifically promoted by interactions with the biomolecule surface.

Analytical ultracentrifugation of the Mb–organoclay nanoparticles showed a single peak with a sedimentation coefficient (s^*) value of 1.5 S, thus indicating a narrow distribution in size and shape of the hybrid structures. The

[*] A. J. Patil, Dr. E. Muthusamy, Prof. S. Mann
School of Chemistry
University of Bristol
Bristol BS8 1TS (UK)
Fax: (+44) 117-929-0509
E-mail: s.mann@bristol.ac.uk

[**] We thank Dr. T. Ikoma (National Institute for Materials Science, Biomaterials Center, Tsukuba, Japan), Dr. D. Scott, Mrs G. Shaw and Dr. A. M. Seddon (University of Bristol) for help with CD spectroscopy, AUC, mass spectroscopy, and enzyme kinetics, respectively. The EPSRC (UK), Max Planck Society, and University of Bristol (ORS award to A.J.P.) are acknowledged for their financial support.

Supporting information for this article is available on the WWW under http://www.angewandte.org or from the author.

  DOI: 10.1002/ange.200453868

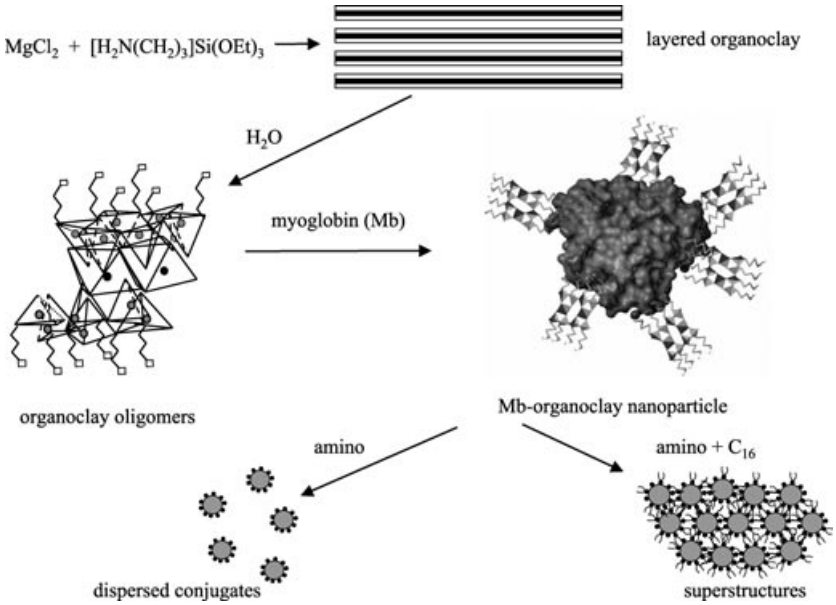

Figure 1. Scheme showing proposed molecular wrapping of Mb molecules by cationic organoclay oligomers with an about 1.6-nm-thick layer structure. Tessellation of the entire protein by binding of the organoclay sheet surface (*ab* face, $a = 0.53$ nm, $b = 0.91$ nm, $\chi = 90°$) requires approximately 30 unit cells. Wrapping with aminopropyl-functionalized organoclay oligomers produces dispersed protein–organoclay nanoparticles, whereas hydrophobic interactions between the exposed C_{16} chains of the aminopropyl/hexadecyl-functionalized oligomers result in nanoparticle self-assembly into partially ordered superstructures.

sedimentation coefficient was reduced compared with native Mb ($s^* = 2.5$ S), which suggests a larger friction coefficient (viscous drag) due to an increase in surface roughness. This was consistent with the proposed core–shell structural model for the organoclay–protein nanoparticles. MALDI-TOF mass spectrometry showed primary peaks for intact Mb (16.9 k) as well as a distribution of organoclay oligomers principally in the mass/charge range of 400 to 700. Studies by using circular dichroism (CD) and FTIR spectroscopies indicated that the secondary structures of Mb, Hb, or GOx molecules were preserved within the organoclay–protein conjugates. For example, CD spectra of solutions of native met-Mb and Mb–organoclay nanoparticles showed characteristic bands[10] for the π–π^* amide transitions at 192 nm and 209 nm, as well as an α-helical n–π^* amide transition at 220 nm (Figure 3a). Similarly, FTIR spectra of the nanoparticles obtained by solvent evaporation showed no changes in the protein amide I (C=O str) and amide II (N–H def, C–N str) bands at 1653 cm^{-1} and at 1554 cm^{-1}, respectively. The spectra also showed absorption bands for CH_2 (2800 cm^{-1}), Si–C (1150 cm^{-1}), Si–O–Si (1025 cm^{-1}), and Mg–O, Si–O, Si–O–Mg (564–482 cm^{-1}) vibrations, confirming that condensed magnesium (aminopropyl)phyllosilicate moieties were associated with the protein/enzyme molecules.

The functional integrity and accessibility of the nanoparticle conjugates to small molecules and ions were assessed by UV/Vis spectroscopy. Solutions of the Mb– or Hb–organoclay nanoparticles showed a distinct $\pi \rightarrow \pi^*$ soret band at 408 nm associated with an intact haem prosthetic group, which showed a characteristic shift to 433 nm on formation, for example, of deoxy-Mb by dithionite reduction (Figure 3b and Supporting Information). Reversible binding of carbon monoxide under argon to the dexoy–Mb(Hb)–organoclay conjugate resulted in a shift in the soret band from 433 nm to 422 nm, which was further shifted after exposure to dioxygen to a value of 416 nm (Figure 3c and Supporting Information), consistent with the formation of oxy–Mb or oxy–Hb.[10] Characteristic changes in the α and β absorption bands at around 580 and 545 nm were also observed. The enzymatic activities of native GOx and GOx–organoclay nanoparticles were monitored spectrophotometrically at 414 nm to determine the initial rates (V) for a range of substrate (S) concentrations (see Experimental Section). In both cases, plots of $1/V$ against $1/[S]$ showed characteristic linear plots consistent with Michaelis–Menton kinetics (Supporting Information). The corresponding values for V_{max} were similar (free GOx, 2.7 $\mu mol\,min^{-1}$; conjugated GOx, 2.95 $\mu mol\,min^{-1}$), thus indicating that the turnover rate at substrate saturation was not significantly affected by interactions with the organoclay. In contrast, the K_m constant associated with the activity of the GOx–organoclay nanoparticles was higher (500 μM) compared with free enzyme (370 μM), which suggests that glucose binding was partially inhibited at intermediate substrate concentrations possibly by restricted diffusion through the organoclay shell of the hybrid conjugate. Measurements of relative enzyme activities at different pH values showed a nonlinear dependence with a small (5–10%) enhancement for the GOx nanoparticles in acid or alkaline conditions compared with the free enzyme in solution (Figure 3d).

The thermal stabilities of organoclay-conjugated met-Mb or Hb molecules were assessed by temperature-dependent UV/Vis spectroscopy measurements of the intensity of the soret band.[16] Compared with room-temperature values, native Mb and Hb showed, respectively, a 49% or 25% reduction in the intensity of the band at 408 nm after 5 min at 85 °C, which is consistent with significant unfolding of the polypeptide chains.[13] In contrast, a decrease of only 10% or 5% in the intensity of the soret band were observed over this temperature range for the met-Mb– or Hb–organoclay nanoparticles, respectively, (Figure 3e), thus indicating a marked increase in thermal stability of the encapsulated protein molecules. Similarly, an increased retention in the activity of GOx–organoclay nanoparticles compared with the native enzyme in solution was observed at elevated temperatures (Figure 3f). Although in both cases, the relative activities were compromised at temperatures above 60 °C, the relative activity of the GOx nanoparticles was at least 10% higher even at 85 °C.

The above results indicate that individual protein/enzyme molecules interact in solution with magnesium (aminopropyl)phyllosilicate oligomers to produce hybrid nanoparticles with preserved protein structure and function, and enhanced

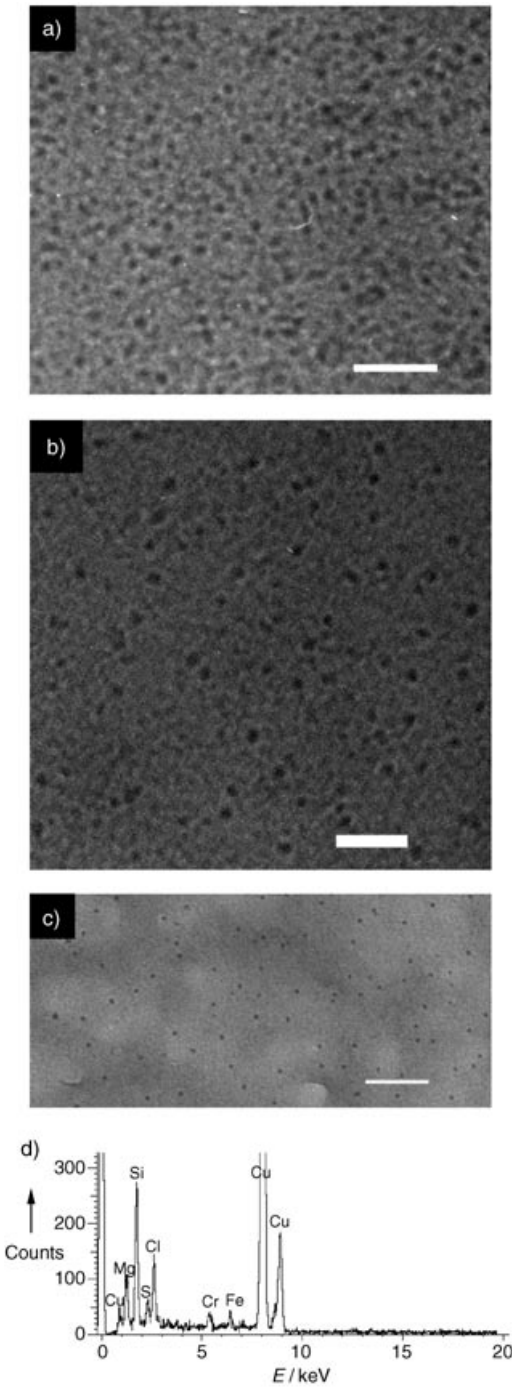

Figure 2. TEM images showing discrete protein-organoclay nanoparticles. a) Mb, b) Hb, and c) GOx.; scale bars = 50, 100, and 100 nm, respectively. d) corresponding EDX analysis for Mb-organoclay nanoparticles. Peaks for Cu and Cr in the EDX spectrum are from the sample holder.

thermal stability. Although further work is required to confirm the proposed structural model and putative wrapping mechanism, electrostatic interactions appear to be in part responsible for conjugation as hybrid nanoparticles were only produced when negatively charged native biomolecules [zeta potential measurements; Mb, −25 mV (pH 8.5); Hb, −26 mV (pH 8.5); GOx, −20 mV (pH 6)] were used in the presence of the positively charged organoclay oligomers (+12 mV (pH 8.5). This mechanism was consistent with the observed absence of hybrid nanoparticles in the presence of cytochrome *c* (zeta potential = +4 mV at pH 8.5), as well as a reduction in the zeta potentials for Mb, Hb, and GOx-containing nanoparticles to values of −18, −0.5 and +1.8 mV, respectively. A similar electrostatic model has recently been proposed to account for the wrapping of viologen polymer molecules within a sheath of partially condensed sodium silicate.[17,18]

Finally, self-assembled superstructures of the Mb–organoclay nanoparticles were produced by replacing about 50% of the aminopropyl groups in the clay structure with covalently attached hydrophobic hexadecyl groups (see Experimental Section). Although the extent of exfoliation was reduced compared with the 100% aminopropyl-functionalized clay, TEM and EDX analysis showed the presence of self-organized protein–organoclay superstructures that consisted of close packed layers of discrete 4.5 nm-sized nanoparticles separated by an interparticle spacing of 4 to 5 nm (Figure 4). This spacing is commensurate with a bilayer of hexadecyl chains as shown from XRD studies of the aminopropyl/hexadecyl magnesium (organo)phyllosilicate clay that revealed an interlayer d_{001} spacing of 4.6 nm (data not shown). The results are consistent with the above structural model in which individual biomolecules are encapsulated by an organoclay shell with pendent organic functionalities, and indicate that macroscopic assemblies of protein–organoclay nanoparticles can be prepared by using interparticle hydrophobic interactions to drive the self-assembly process. Preservation of protein structure and function in these organized hybrid materials was confirmed by using the above experimental procedures (see the Supporting Information).

In conclusion, we have demonstrated that novel organoclay–protein conjugates can be prepared in the form of discrete electron-dense nanoparticles. On the basis of our results, we propose a core–shell structural model in which individual biomolecules are wrapped by an inorganic shell of condensed organoclay oligomers. The procedure is facile and could lead to new types of stabilized biomolecules that can be functionally isolated as discrete soluble units, or assembled and integrated into nanostructured materials. In particular, the use of "armour-plated" proteins should circumvent problems arising from the loss of functional isolation associated with adverse intermolecular interactions within interconnected networks of biomolecules. In addition, the enhanced thermal and chemical stability of inorganically wrapped proteins should markedly increase the scope for using protein-based nanostructures in areas such as tissue engineering and biomolecular sensing.

Experimental Section

Organoclay synthesis and exfoliation: Typically, an aminopropyl-functionalized magnesium (organo)phyllosilicate clay was prepared at room temperature by dropwise addition of 3-aminopropyltriethoxysilane (1.3 mL, 5.85 mmol) to an ethanolic solution of magnesium chloride (0.84 g, 3.62 mmol) in ethanol (20 g). The white slurry obtained after 5 min was stirred overnight and the precipitate isolated

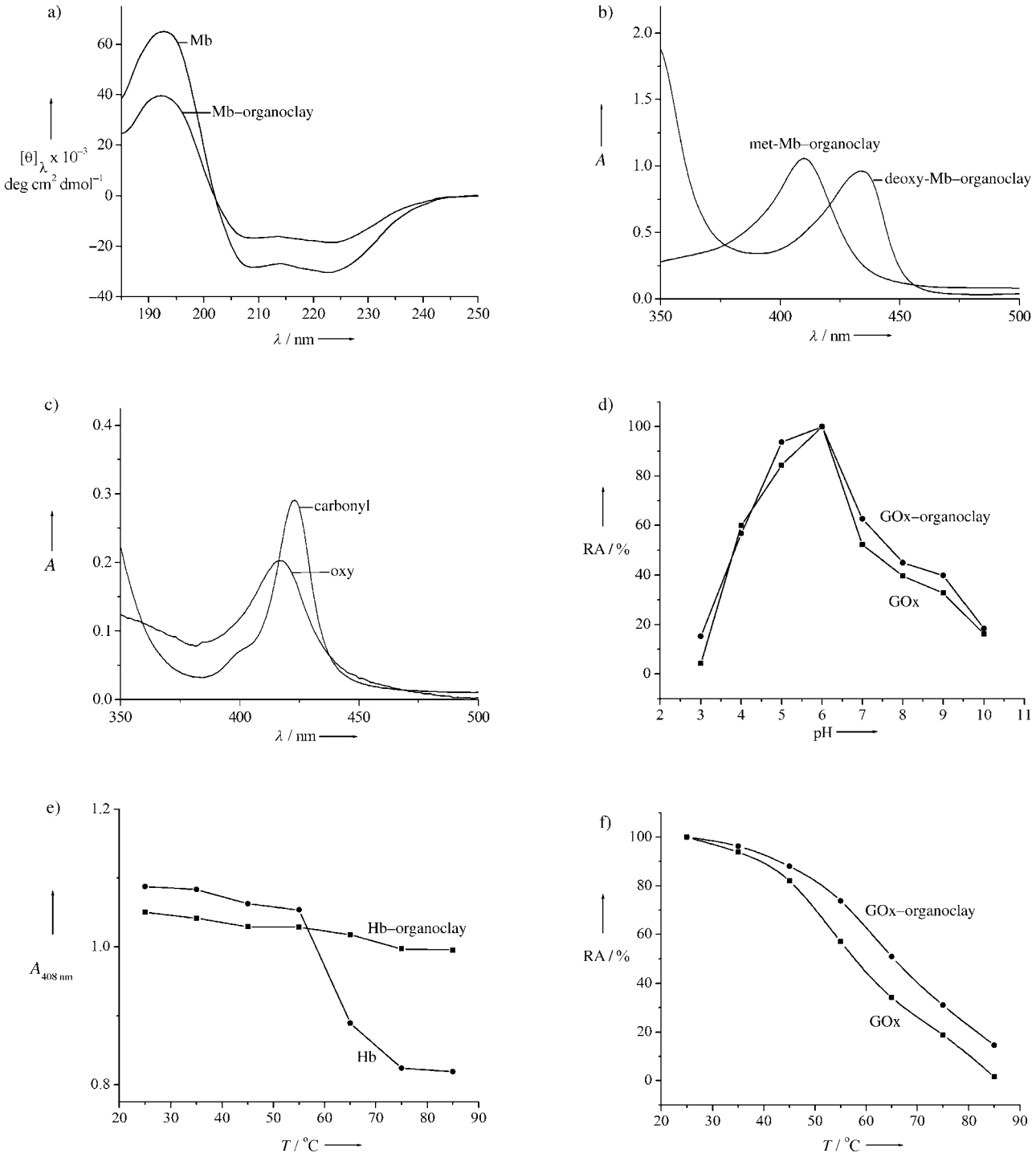

Figure 3. a) CD spectra of solutions of native Mb and Mb–organoclay nanoparticles that show π–π* amide α-helical n–π* amide transitions corresponding to intact secondary structures. b) UV/Vis spectra of met-Mb–organoclay conjugates that show soret band absorptions for as-prepared nanoparticles and after dithioinite reduction and formation of deoxy-Mb. c) UV/Vis spectra of Mb–organoclay nanoparticles after CO binding to the deoxy-protein and subsequent O_2 binding and formation of oxy-Mb. d) Plot of relative activity (RA, %) against pH for native GOx (■) and GOx–organoclay nanoparticles (●). e) Plots of absorbance intensity at 408 nm (A_{408}) with temperature for solutions of native Hb (●) and Hb–organoclay nanoparticles (■), showing increased thermal stability of the wrapped protein molecules. Samples were allowed to stand for 5 min at each temperature prior to analysis. f) Plot of relative activity (%) against temperature for native GOx (■) and GOx–organoclay nanoparticles.

by centrifugation, washed with ethanol (50 mL) and dried at 40 °C. Exfoliation of the clay was undertaken by dispersing 10 mg of the dried clay in distilled water (10 mL) followed by ultrasonication for 5 mins. The resulting cloudy dispersion was passed through a sephadex G-25/75 column (Aldrich), and the clear eluate collected and used for experiments with a range of biomolecules.

Organoclays consisting of covalently linked aminopropyl and long-chain hexadecyl groups were prepared by addition with constant

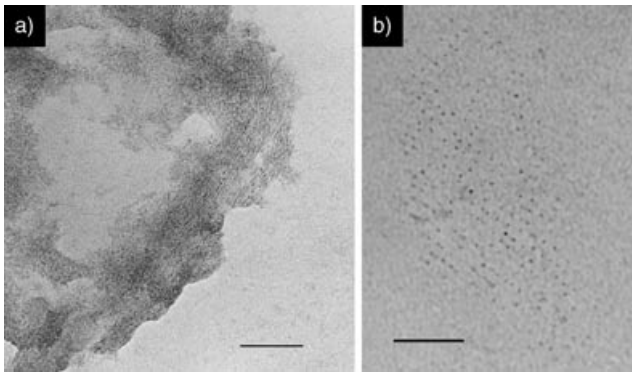

Figure 4. a) TEM image showing self-organized layers of Mb molecules wrapped by magnesium (aminopropyl/hexadecyl)phyllosilicate oligomers. The lamellar structure is viewed side-on such that the interlayer spacing of the superstructure is clearly revealed (arrow); scale bar = 100 nm. b) Corresponding image of a single layer viewed from above showing the presence of superstructural ordering of the protein–organoclay hydrophobic nanoparticles; scale bar = 50 nm.

stirring of a 1:1 molar ratio mixture of hexadecyltrimethoxysilane (1.80 mmol) and 3-aminopropyltriethoxysilane (1.80 mmol) in ethanol (10 g) to magnesium chloride (0.25 g, 1.08 mmol) dissolved in ethanol (10 g), followed by addition of aqueous sodium hydroxide (0.5 M, 20 mL). The reaction mixture was stirred for 24 h at room temperature, after which a finely divided white precipitate was collected by vacuum filtration and washed repeatedly with water and ethanol then dried at 40 °C in air for 24 h. Exfoliation of the bifunctional clay was undertaken by dispersion of 10 mg of a finely ground sample in a water/ethanol (15 mL/5 mL) mixture by ultrasonication for 2 min. (Exfoliation was not successful in pure water due to the highly hydrophobic character of the organoclay particles).

Protein-organoclay nanoparticles: A purified met-Mb aqueous solution (1 mL, 12.4 μM, horse skeletal muscle (sigma), $M_r = 16.9$k, sephadex G-25/75) was added dropwise to the amino-functionalized organoclay eluate (2 mL) to give a clear reddish-brown solution of pH ≈ 8.5 of the clay-wrapped protein molecules, which became slightly turbid when left at room temperature for up to 24 h. Similar procedures were also undertaken with purified Hb (1 mL, 47 μM, bovine (sigma), $M_r = 64$k, sephadex G-25/75) and GOx (1 mL, 10 μM, *Aspergillus niger*, type X-S, EC 1.1.3.4, $M_r = 140$k, pH 6) aqueous solutions.

Alternatively, an Mb aqueous solution (1 mL, 10 mg mL^{-1}) was added to the exfoliated dispersion of an aminopropyl/hexadecyl-functionalized organoclay and stirred at room temperature for 5 days at pH ≈ 8.5. The precipitate obtained was centrifuged, washed with water and dried at room temperature for two days.

Reduction of met-Mb (or met-Hb) to the deoxy form was undertaken by treating native Mb (10 mL, 0.10 mg mL^{-1}) or Mb-organoclay nanoparticles with sodium dithionite (1 mg) under an argon atmosphere. Binding of carbon monoxide to dexoxy-Mb or deoxy-Mb–organoclay conjugate solutions prepared by dithionite reduction was undertaken by purging CO gas through the sample solutions for one hour at room temperature. Subsequent exchange of bound CO by dioxygen was undertaken by passing solutions of the carbonyl-Mb through a sephradex gel column in air.

The rates of oxidation of β-D-glucose to D-gluconolactone and H_2O_2 by native and organoclay-wrapped GOx were determined spectrophotometrically.[19] Decomposition of H_2O_2 in the presence of horse radish peroxidase (HRP, type II, sigma) and an electron donar dye, 2,2′-azino-bis(3-ethylbenzethiazoline-6-sulfonic acid (ABTS, sigma) was monitored by increases in absorption at 414 nm (A_{414}) associated with formation of oxidized ABTS. Typically, reactions were carried out at 25 °C in 3 mL glass cuvettes at pH 6 by addition of native GOx oxidase or GOx–organoclay nanoparticles (100 μL, [GOx] = 10 μM] to sodium phosphate buffered solutions (1.6 mL, 0.1 M) containing 100 μL of ABTS (50 mM)/HRP (2.6 μM, 25 units mL^{-1}) and β-D-Glucose (concentration range, 3.5 μM to 50 μM). Changes in A_{414} with time were converted to units of enzyme specific activity (μmol min^{-1} mg^{-1}) by using an extinction coefficient of 3.6×10^4 M^{-1} cm^{-1}. Double reciprocal plots of $1/V$ (V = initial rate) against 1/[glucose] showed linear behavior consistent with Michaelis–Menton kinetics, and the Michaelis constant (K_M) and maximal rate (V_m) were determined directly from the plots. The above procedure was also carried out with native and organoclay-wrapped GOx under a range of pH values (3 to 10) and temperatures (25 and 85 °C). In each case, the specific activities of free GOx or GOx-organoclay nanoparticles were converted into percentage relative activities based on corresponding values obtained at pH 6 and 25 °C.

The thermal stabilities of native Mb/Hb and Mb/Hb–organoclay nanoparticles were determined by temperature-dependent UV/Vis spectroscopy (Perkin Elmer Lambda II) by using an attached Peltier temperature-control system and monitoring changes in the absorbance intensity of the 408 nm soret band of samples allowed to stand for 5 mins at temperatures between 35 and 85 °C. Temperature-dependent enzyme activities of free GOx and GOx–organoclay conjugates were also determined by using the Peltier control system. Samples were incubated for 5 mins at temperatures between 25 to 85 °C before measuring changes in absorbance changes at 414 nm.

Samples were characterized by TEM (JEOL 1200EX), EDX analysis (Oxford Instruments, ISIS300), and XRD (Bruker-Nonius D8 diffractometer, $Cu_{K\alpha}$ radiation, $\lambda = 0.15405$ nm). FTIR spectroscopy (Perkin Elmer Spectrum 1) was carried out by using KBr discs. CD spectra were measured at 298 K by using a JASCO model 725 spectrometer with a quartz cell and path length of 10 mm at a scan speed of 50 nm min^{-1}. Zeta potential measurements were undertaken by using a Zetaplus analyser. Analytical ultracentrifugation was carried out by using a Beckman Analytical Centrifuge at 40000 rpm. MALDI-TOF mass spectrometry (PE Biosystems Voyager-DE STR) was undertaken using a nitrogen laser operating at 337 nm. Samples and matrix (0.5 μL each) were spotted onto a sample plate and calibrated against "Calmix 3" (PE, Biosystems) as external standard. The matrix solution was freshly prepared sinapinic acid (Fluka) at a concentration of 1 mg/100μL in a 50:50 mixture of acetonitrile/0.1 % TFA.

Received: January 27, 2004
Revised: April 26, 2004 [Z53868]

Keywords: biological activity · nanoparticles · organic-inorganic hybrid composites · self-assembly

[1] T. O. Yeates, J. E. Padilla, *Curr. Opin. Struct. Biol.* **2002**, *12*, 464 – 470.
[2] T. C. Holme, *Trends Biotechnol.* **2002**, *20*, 16 – 24.
[3] J. D. Hartgerink, E. Beniash, S. I. Stupp, *Proc. Natl. Acad. Sci. USA* **2002**, *99*, 5133 – 5138.
[4] M. Jiang, B. Nolting, P. S. Stayton, S. G. Sligar, *Langmuir* **1996**, *12*, 1278 – 1283.
[5] Y. Zhou, N. Hu, Y. Zeng, J. F. Rusling, *Langmuir* **2002**, *18*, 211 – 219.
[6] V. Panchagnula, C. V. Kumar, J. F. Rusling, *J. Am. Chem. Soc.* **2002**, *124*, 12515 – 12521.
[7] M. Onda, A. Katsuhiko, T. Kunitake, *J. Biosci. Bioeng.* **1999**, *87*, 69 – 75.
[8] F. Caruso, C. Schuler, *Langmuir* **2000**, *16* 9595 – 9603.
[9] I. Gill, A. Ballesteros, *Trends Biotechnol.* **2000**, *18*, 282 – 296.
[10] L. M. Ellerby, C. R. Nishida, F. Nishida, A. Yamanaka, B. Dunn, J. S. Valentine, J. Zink, *Science* **1992**, *255*, 1113 – 1115.

[11] Q. Gao, S. L. Suib, J. F. Rusling, *Chem. Commun.* **2002**, 2254 – 2254.
[12] C. V. Kumar, A. Chaudhari, *J. Am. Chem. Soc.* **2000**, *122*, 830 – 837.
[13] C. V. Kumar, A. Chaudhari, *Chem. Commun.* **2002**, 2382 – 2383.
[14] S. L. Burkett, A. Press, S. Mann, *Chem. Mater.* **1997**, *9*, 1071 – 1073.
[15] N. T. Whilton, S. L. Burkett, S. Mann, *J. Mater. Chem.* **1998**, *8*, 1927 – 1932.
[16] G. Acampora, J. Hermans, *J. Am. Chem. Soc.* **1967**, *89*, 1543 – 1547.
[17] I. Ichinose, T. Kunitake, *Chem. Rec.* **2002**, *2*, 339 – 351.
[18] I. Ichinose, T. Kunitake, *Adv. Mater.* **2002**, *14*, 344 – 346.
[19] R. C. Bateman, J. A. Evans, *J. Chem. Educ.* **1995**, *72*(12), A240 – A241.

